

Acetyl Radical Production by the Methylglyoxal–Peroxynitrite System: A Possible Route for L-Lysine Acetylation

Júlio Massari,^{†,‡} Rita Tokikawa,[†] Luiz Zanolli,[‡] Marina Franco Maggi Tavares,[‡] Nilson Antônio Assunção,[§] and Etelvino José Henriques Bechara^{*,†,§}

Departamento de Bioquímica and Departamento de Química Fundamental, Instituto de Química, Universidade de São Paulo, São Paulo, SP, Brazil, and Departamento de Ciências Exatas e da Terra, Universidade Federal de São Paulo, Diadema, SP, Brazil

Received July 1, 2010

Methylglyoxal is an α -oxoaldehyde putatively produced in excess from triose phosphates, aminoacetone, and acetone in some disorders, particularly in diabetes. Here, we investigate the nucleophilic addition of ONOO⁻, known as a potent oxidant and nucleophile, to methylglyoxal, yielding an acetyl radical intermediate and ultimately formate and acetate ions. The rate of ONOO⁻ decay in the presence of methylglyoxal [$k_{2,app} = (1.0 \pm 0.1) \times 10^3 \text{ M}^{-1} \text{ s}^{-1}$; $k_2 \approx 1.0 \times 10^5 \text{ M}^{-1} \text{ s}^{-1}$] at pH 7.2 and 25 °C was found to be faster than that reported with monocarbonyl substrates ($k_2 < 10^3 \text{ M}^{-1} \text{ s}^{-1}$), diacetyl ($k_2 = 1.0 \times 10^4 \text{ M}^{-1} \text{ s}^{-1}$), or CO₂ ($k_2 = 3\text{--}6 \times 10^4 \text{ M}^{-1} \text{ s}^{-1}$). The pH profile of the methylglyoxal–peroxynitrite reaction describes an ascendant curve with an inflection around pH 7.2, which roughly coincides with the pK_a values of both ONOOH and H₂PO₄⁻ ion. Electron paramagnetic resonance spin trapping experiments with 2-methyl-2-nitrosopropane revealed concentration-dependent formation of an adduct that can be attributed to 2-methyl-2-nitrosopropane-CH₃CO[•] ($a_N = 0.83 \text{ mT}$). Spin trapping with 3,5-dibromo-4-nitrosobenzene sulfonate gave a signal that could be assigned to a methyl radical adduct [$a_N = 1.41 \text{ mT}$; $a_H = 1.35 \text{ mT}$; $a_{H(m)} = 0.08 \text{ mT}$]. The 2-methyl-2-nitrosopropane-CH₃CO[•] adduct could also be observed by replacement of ONOO⁻ with H₂O₂, although at much lower yields. Acetyl radicals could be also trapped by added L-lysine as indicated by the presence of ⁶N-acetyl-L-lysine in the spent reaction mixture. This raises the hypothesis that ONOO⁻/H₂O₂ in the presence of methylglyoxal is endowed with the potential to acetylate proteins in post-translational processes.

Introduction

Methylglyoxal (MG) is a highly reactive α -oxoaldehyde putatively produced in vivo by three distinct enzymatic routes [(i) formation from triose phosphates, (ii) cytochrome P450 IIE1-catalyzed acetone oxidation, and (iii) amine oxidase(s)-driven amino acid breakdown] as well as by nonenzymatic pathways from glucose, triose phosphates, acetoacetate, succinylacetone, and aminoacetone (1–9). Exogenous sources of MG include many food products, beverages, fog and rainwater, urban atmosphere, and cigarette smoke (10). Although MG is normally consumed by glyoxalases, aldehyde oxidases, and other enzymes, MG undergoes biologically adverse nucleophilic additions and promotes protein aggregations that are purportedly involved in diabetes, Alzheimer's disease, and other age-related diseases (3, 4). Nanomolar to micromolar concentrations of free MG have been reported in normal human plasma (4), the variability being probably related to conjugation of MG with proteins and to different methods used in sample preparation and analysis (4, 11). According to Beisswenger et al. (12), the concentration of MG in blood plasma of normal human subjects

is $123 \pm 37 \text{ nM}$ and in type 2 diabetics $189.3 \pm 38.7 \text{ nM}$, while cellular concentrations of MG were in the range of 1–5 μM (4).

The high reactivity of MG and other dicarbonyl metabolites (e.g., diacetyl, 4,5-dioxovaleric acid, and osazones) to biological nucleophiles (e.g., basic amino acids, DNA bases, and thiols) lies in the electron withdrawing effect of a vicinal carbonyl group, which increases the electrophilicity of the adjacent carbonyl moiety, thereby facilitating nucleophilic attack. Accordingly, MG has been found in aqueous solutions as a mixture of hydrated derivatives in dynamic equilibrium, where MG monohydrate (56–62%) and dihydrate (38–44%) forms prevail and only traces of the free form are observed (13). Experiments conducted by Thornalley and co-workers with MG in 50 mM sodium phosphate buffer (pH 7.4) at 37 °C revealed the approximate ratio of these forms of 28:71:1 (MG monohydrate:MG dihydrate:free MG) (14).

The higher reactivity of α -dicarbonyls, particularly MG, compared to that of monocarbonyls, explains the recently reported k_2 value for the addition of peroxynitrite anion to diacetyl ($\approx 10^4 \text{ M}^{-1} \text{ s}^{-1}$) (15, 16) that is 1 order of magnitude higher than that of monocarbonyls ($< 10^3 \text{ M}^{-1} \text{ s}^{-1}$) (16–18). In addition to being a powerful nucleophile, peroxynitrite can directly or indirectly drive one- and two-electron oxidations, nitrosations, and nitrations of biomolecules, of which a number of final products have been detected and adopted as biomarkers of disorders. The detection of these products in biological samples allows them to be linked with the clinical manifestations of various maladies such as Alzheimer's disease, rheumatoid

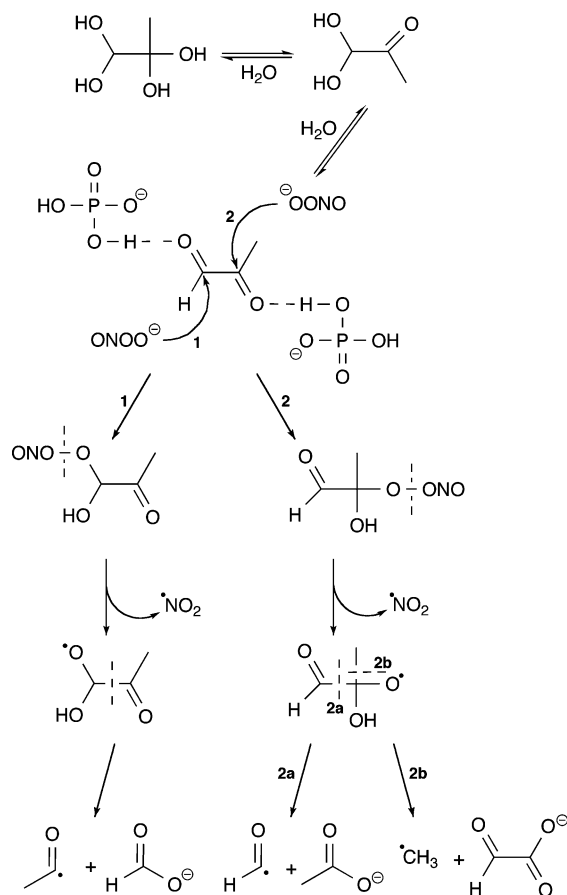
* To whom correspondence should be addressed: Departamento de Bioquímica, Instituto de Química, Universidade de São Paulo, Av. Prof. Lineu Prestes, 748, 05508-900 São Paulo, SP, Brazil. Phone: 55-11-30913869. Fax: 55-11-38155579. E-mail: ebechara@iq.usp.br.

[†] Departamento de Bioquímica, Instituto de Química, Universidade de São Paulo.

[‡] Departamento de Química Fundamental, Instituto de Química, Universidade de São Paulo.

[§] Universidade Federal de São Paulo.

Scheme 1. Hypothetical Mechanism Pathways for the Peroxynitrite-Initiated Aerobic Oxidation of MG in an Aqueous Medium to Formate and Acetate Ions, Mediated by Acetyl Radical^a



^a The data obtained from kinetic, product, and spectroscopic analyses favor route 1, predicted by the long-known higher reactivity of aldehydes with nucleophiles compared to that of ketones.

arthritis, atherosclerosis, lung injury, amyotrophic lateral sclerosis, diabetes, cancer, and drug-dependent toxicity (19–28).

Recently, when revisiting the nucleophilic addition of peroxynitrite to diacetyl, first studied by Yang et al. (16), we demonstrated large amounts of acetyl radical intermediate in the reaction mixture allowing coupled acetylation of added L-histidine or 2'-deoxyguanosine (dGuo) (15). On the basis of previous work by Pryor's group (17) and Augusto's group (18), the mechanism underlying acetyl radical production was envisaged as being initiated by nucleophilic attack of peroxynitrite on diacetyl yielding a hypothetical nitrosoperoxydiacetyl intermediate, whose homolysis yields nitrogen dioxide and an oxyl radical. The latter then undergoes β -cleavage producing two fragments, acetate anion and acetyl radical, whose fate can be direct oxidation by dissolved dioxygen, ultimately yielding acetate anion, or addition to L-His or dGuo, forming the corresponding acetylated compounds (Scheme 1). In vivo, more than 99% of produced MG may be consumed by proteins via Schiff additions to arginine and lysine residues (29, 30). Knowing that enzymatic post-translational acetylations and deacetylations of proteins regulate key cellular events (31), the authors raised the hypothesis that diacetyl- or MG-triggered radical acetylation in vivo might contribute to these epigenetic processes.

We show here that MG reacts with peroxynitrite 10-fold faster than does diacetyl and may eventually compete with HCO_3^-

CO_2 as an electrophilic target in the peroxynitrite reaction, although one should keep in mind the fact that the concentration of bicarbonate in tissues is 4 orders of magnitude higher than that of MG (4, 21). Acetyl radical, produced by MG-oxyl radical homolysis, and methyl radical, probably formed from decarbonylation of acetyl radical, were captured by electron spin paramagnetic resonance (EPR) using appropriate spin traps. Acetate and formate are expectedly the main reaction products. Finally, previous addition of L-lysine to the reaction mixture yielded the corresponding ^εN-acetylated amino acid.

Materials and Methods

Chemicals and Reagents. HPLC grade acetonitrile, ammonium formate, cetyltrimethylammonium bromide (CTAB), Chelex-100, 3,5-dinitrobenzoic acid (DNB), 2,4-dinitrophenylhydrazine, HPLC grade methanol, 2-methyl-2-nitrosopropane dimer (MNP), a 40% aqueous methylglyoxal (MG) solution, H_3PO_4 , and NaNO_2 were purchased from Sigma-Aldrich (St. Louis, MO). Acetic acid, HCl, H_2O_2 , MnO_2 , NaOH, $\text{Na}_2\text{HPO}_4 \cdot 12\text{H}_2\text{O}$, and $\text{NaH}_2\text{PO}_4 \cdot \text{H}_2\text{O}$ were supplied by Merck (Darmstadt, Germany). L-Lysine-HCl was acquired from Fluka (Buchs, Switzerland). The spin trap 3,5-dibromo-4-nitrosobenzenesulfonic acid (DBNBS) was synthesized as previously described (32). Peroxynitrite was synthesized from NaNO_2 (0.60 M) and H_2O_2 (0.70 M), in HCl (0.60 M) and NaOH (1.50 M) in a quench-flow reactor (33). Excess H_2O_2 in the alkali peroxynitrite solution was eliminated with MnO_2 . Concentrations of H_2O_2 and peroxynitrite were determined spectrophotometrically at 240 ($\epsilon = 42 \text{ M}^{-1} \text{ cm}^{-1}$) (34) and 302 nm ($\epsilon = 1670 \text{ M}^{-1} \text{ cm}^{-1}$) (33, 35), respectively. The peroxynitrite concentrations obtained by this method ranged from 300 to 450 mM. Stock solutions of peroxynitrite were kept on ice in the dark. All the solutions were prepared in Millipore Milli-Q purified water, and the buffers were pretreated with Chelex-100 to remove metal contaminants. Methylglyoxal stock solutions were determined by previous derivatization with 2,4-dinitrophenylhydrazine in MeOH-HCl for 40 min at 42 °C, which yields an adduct measured at 432 nm ($\epsilon = 39300 \text{ M}^{-1} \text{ cm}^{-1}$) (36).

Stopped-Flow Kinetics. The rate of peroxynitrite decay was monitored with a stopped-flow spectrophotometer (Applied Photophysics model SX-18 V) at 302 nm. The temperature was kept constant at 25.0 ± 0.2 °C, and the pH values of the reaction mixtures were determined by a simulated experiment in Eppendorf tubes under the same conditions. The initial concentration of peroxynitrite was kept at 200 μM . Pseudo-first-order rates, k_{obs} (s^{-1}), were determined by linear fit from $\ln A$ versus time (0–30 ms). The results of 9–12 measurements were averaged to yield each rate constant. The apparent second-order rate constant ($k_{2,\text{app}}$) was calculated from slopes of the plots of k_{obs} versus MG concentration. The rate of peroxynitrite decay in the buffer solution, k_0 , was subtracted from k_{obs} before the data were plotted versus pH or phosphate buffer concentration. All the data were fit using Origin 7 (Microcal Software, Inc.).

EPR Spin Trapping Experiments. EPR spin trapping spectra with MNP were recorded at room temperature using a Bruker EMX spectrometer. All of the spectra were recorded after incubation of the reagents for 4 min, except when the spin trap was DBNBS (2 min), in 250 mM phosphate buffer (pH 7.2). At the end of the experiment, the pH was measured to detect possible changes caused by the addition of alkaline stock solutions of peroxynitrite to the buffered reaction mixtures. The instrumental conditions were as follows: microwave power, 20.17 mW; modulation amplitude, 0.1 mT; time constant, 163.840 ms; and receiver gain, 2.52×10^4 for experiments conducted with MG, peroxynitrite, MNP, and bicarbonate and 2.52×10^5 for experiments with DBNBS as the spin trap or MG, H_2O_2 , and MNP.

Oxygen Consumption. Oxygen uptake was monitored in a Hansatech oxygraph equipped with a Clark type electrode. All the experiments were conducted in air-equilibrated 200 mM phosphate buffer (pH 7.2) at 25 °C.

Capillary Electrophoretic Analysis. The electropherogram traces for carboxylic acids were obtained with a system (model P/ACE 551) from Beckman Instruments (Fullerton, CA) equipped with a filter-carrousel UV detector set at 254 nm for indirect detection, with the temperature control device maintained at 25 °C. The background electrolyte was 10 mM DNB, with 0.10 mM CTAB, and the final pH was 3.6. Fused-silica capillaries (Polymicro Technologies, Phoenix, AZ) with dimensions of 50.0 cm (total length) (40 cm effective length), 50 μm (inside diameter), and 375 μm (outside diameter) were used. Separation was performed at a constant voltage (-20 kV). Samples were injected hydrodynamically with 1 psi for 3 s. Aliquots of peroxyxynitrite and phosphoric acid (2.5–11.0 mM), sufficient to obtain a final pH ranging from 7.1 to 7.5, were added to the millimolar MG-containing solution, which was stirred vigorously in a Vortex system before capillary electrophoresis (CE) measurements were taken. Oxalic acid was used as an internal standard, and the reaction mixture was analyzed immediately.

CE-MS/MS Analysis. All analyses were performed with a P/ACE MDQ system from Beckman Instruments, coupled to a Thermo Finnigan mass spectrometer (MS), a model LCQ Ion Max Advanced with an electron spray ion source, and an ion trap analyzer from Thermo Electron Corp. (Walther, MA). The sheath liquid (50:49.5:0.5 methanol/water/acetic acid mixture) was pumped (5 $\mu\text{L}/\text{min}$) into the interface with a syringe from Hamilton (Reno, NV) installed in the MS. An uncoated fused-silica capillary from

Polymicro Technologies (Phoenix, AZ) was used (total length of 90 cm and inside diameter of 50 μm). Separation was performed at a constant voltage (25 kV). The separation buffer was 50 mM ammonium acetate (pH 3.5). The CE capillary was preconditioned with 1.00 M NH_4OH , deionized water, and finally separation buffer for 5 min in each step at a pressure of 50 psi. Samples were injected hydrodynamically (injection time of 10 s at 2 psi). Experimental MS and MS/MS conditions were as follows: number of microscans, 3; microscan time, 200 ms; capillary temperature, 275 °C; spray voltage, 27 V; and tube lens offset, -8 V. MS/MS experiments were conducted in the positive ion mode at an ion spray voltage of 4.5 kV. Mass spectrometry tuning was performed with Xcalibur 1.4 SR1 (Thermo Electron Corp.) using a direct infusion of 20 μM L-lysine at a pressure of 10 psi. Data acquisition was performed by MS/MS scans at the most intense peaks with the normalized collision energy for MS/MS set to 35% and an isolation width of m/z 1.0. A minimal signal intensity threshold of 1×10^3 was set for the acquisition of the MS/MS data. Nitrogen was used as a nebulization and sweep gas at flow rates of 15 and 5 arbitrary units, respectively, and helium was used for the fragmentation process.

Results

Peroxyxynitrite Decay. Time courses of the consumption of peroxyxynitrite (200 μM) by MG (0–20 mM), monitored at 302 nm, are shown in Figure 1A. The pseudo-first-order rate

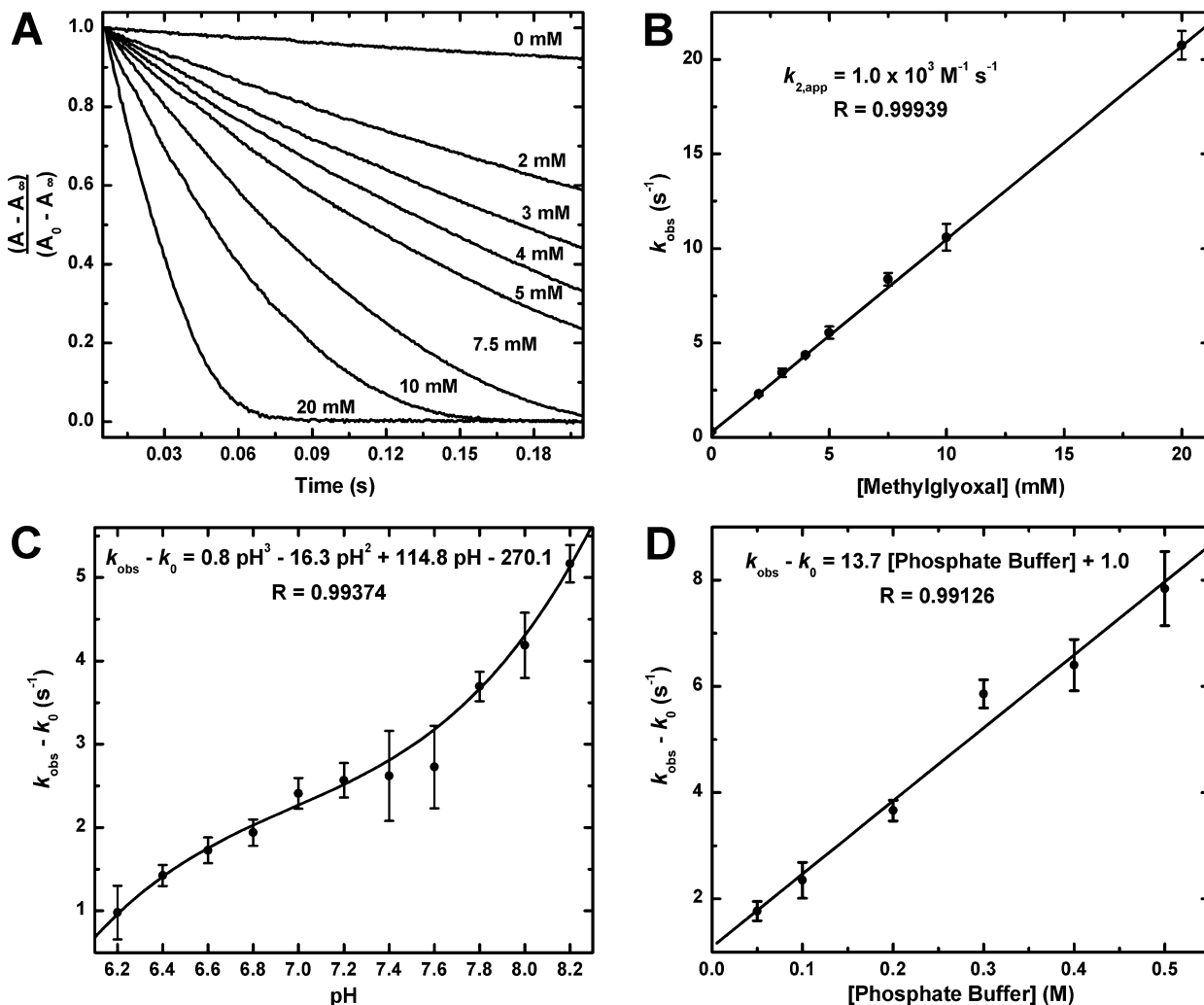


Figure 1. Stopped-flow kinetics of peroxyxynitrite decay in the presence of MG. (A) Kinetic traces of peroxyxynitrite (200 μM) decay at different MG concentrations (0–20 mM) in air-equilibrated 250 mM phosphate buffer (pH 7.2) at 25 °C. (B) Pseudo-first-order rate constants (k_{obs}) for the decay of peroxyxynitrite in the presence of MG under the same experimental conditions. Each k_{obs} value represents the mean of nine measurements. (C) pH profile of the reaction of MG (3.0 mM) with peroxyxynitrite (200 μM) in air-equilibrated 250 mM phosphate buffer at 25 °C. (D) Catalytic effect of phosphate anion on the observed rate of peroxyxynitrite (200 μM) treated with MG (4.0 mM) at pH 7.2 and 25 °C. The ionic strength of the phosphate buffer was kept constant via the addition of sodium chloride. The data represent the means of nine independent measurements.

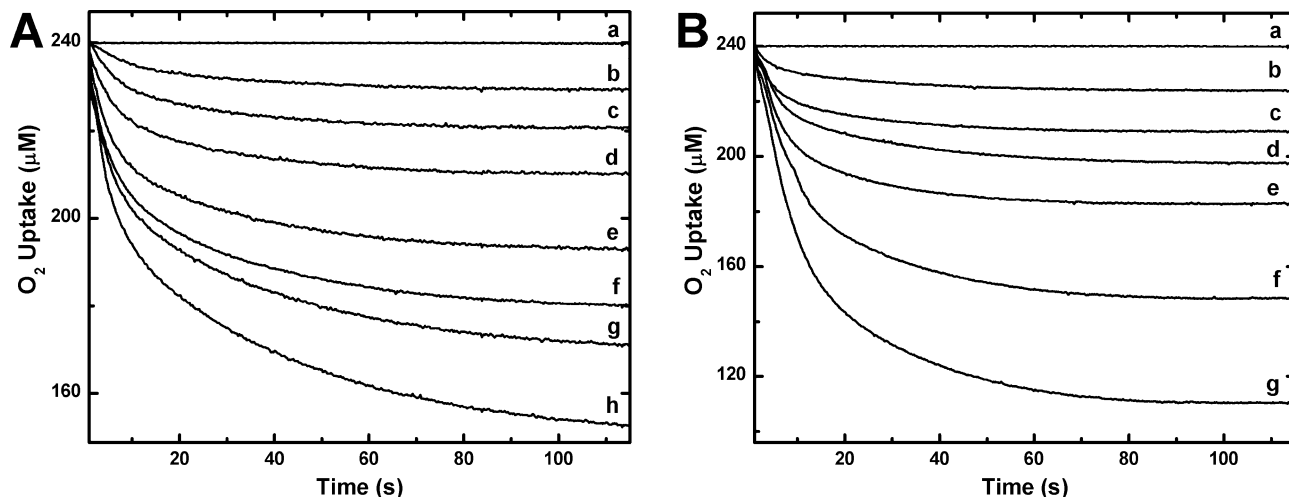


Figure 2. Time courses of uptake of oxygen by MG treated with peroxynitrite, in 200 mM phosphate buffer (pH 7.2) at 25 °C. (A) MG (1.0 mM) in the absence of peroxynitrite (a) and 0.05 (b), 0.10 (c), 0.25 (d), 0.50 (e), 1.00 (f), 1.50 (g), and 2.50 mM MG (h) treated with 1.0 mM peroxynitrite. (B) MG (1.0 mM) in the absence (a) and presence of 0.25 (b), 0.50 (c), 0.75 (d), 1.00 (e), 1.50 (f), and 2.00 mM peroxynitrite (g).

constants (k_{obs}) were found to increase linearly with the initial concentration of MG, revealing an apparent second-order rate constant ($k_{2,\text{app}}$) equal to $(1.0 \pm 0.1) \times 10^3 \text{ M}^{-1} \text{ s}^{-1}$ (mean value of three independent $k_{2,\text{app}}$ determinations) in 250 mM phosphate buffer (pH 7.2) at 25 °C (Figure 1B). Because (i) <1% of dissolved MG is present in the free ketoaldehyde form due to extensive MG hydration (13, 14) and (ii) the phosphate-catalyzed MG diol dehydration is a very slow process ($k_{\text{d}} = 7.7 \times 10^{-2}$ and $5.7 \times 10^{-1} \text{ M}^{-1} \text{ s}^{-1}$ for general acid and general base phosphate catalysis, respectively, at 25 °C, $\mu = 0.2 \text{ M}$) (37), the actual value of k_2 must be corrected by the expression $k_2 = k_{2,\text{app}}(1 + \text{unreactive forms/keto aldehyde form})$ (16), which gives a k_2 value of $\approx 1.0 \times 10^5 \text{ M}^{-1} \text{ s}^{-1}$ assuming free MG as 1% of the nominal MG concentration. This value is 2 orders of magnitude higher than that observed for monocarbonyls (17, 18), 10-fold higher than that with diacetyl (15, 16), and 2–3 times higher than the rate constant reported for $\text{HCO}_3^-/\text{CO}_2$ at pH 7.2–7.4 and 25–37 °C ($3\text{--}6 \times 10^4 \text{ M}^{-1} \text{ s}^{-1}$) (21, 38–40). The pH profile of the MG–peroxynitrite reaction, monitored in the pH range of 6.2–8.2, obeys a third-degree equation, displaying a shoulder at pH 7.2 (Figure 1C). Going from pH 6.2 to 7.2, the ascendant curve may be attributed to an increasing concentration of the nucleophile (peroxynitrite), and the concomitant decrease of the H_2PO_4^- anion concentration, which catalyzes the nucleophilic addition to MG (14). The sharper increase in the curve above pH 7.2 may be due to dehydration of MG diol to its free, reactive carbonyl form, catalyzed by the monophosphate anion, as suggested by Thornalley et al. (14) in their study of addition of aminoguanidine to MG, a much slower reaction ($k_2 = 178 \text{ M}^{-1} \text{ s}^{-1}$ at pH 7.4 and 37 °C) (14). The occurrence of general base catalysis by phosphate anion in the reaction of MG with peroxynitrite is supported by the linear dependence of k_{obs} on phosphate buffer concentration (0.05–0.50 M; pH 7.2) (Figure 1D).

Oxygen Uptake and Product Analysis. Addition of peroxynitrite to MG is expected to be followed by rearrangement of a peroxynitroso adduct to re-formed MG and nitrate ion, in parallel with adduct homolysis to a MG-derived oxyl radical that ultimately produces formate and acetyl radical by β -cleavage (15–18). Annihilation of acetyl radical by dissolved dioxygen would lead to acetate ion as a side product. Accordingly, uptake of oxygen by the MG (0.05–2.5 mM)–peroxynitrite (0.25–2.0 mM) system was found to occur in a reagent concentration-dependent fashion (Figure 2). Control experiments

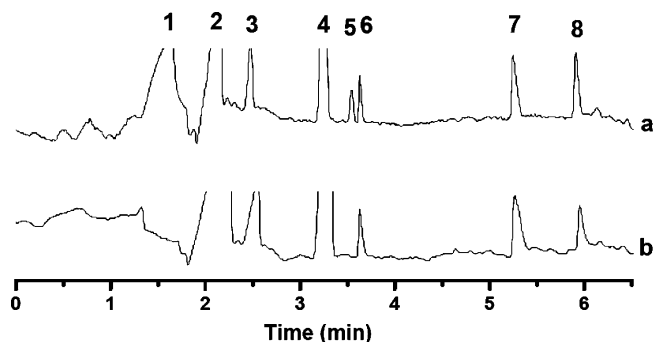


Figure 3. CE of the reaction products of MG treated with peroxynitrite. Electropherograms of a standard mixture (a) and the final reaction mixture of 1.00 mM MG, treated with 1.00 mM peroxynitrite and 2.75 mM phosphoric acid, with the final pH ranging from 7.2 to 7.5 (b). Peak identification: (1) system peak, (2) nitrite, (3) nitrate, (4) phosphate, (5) glyoxalate, (6) formate, (7) oxalate (internal standard), and (8) acetate. Experimental conditions: 10 mM DNB with 0.10 mM CTAB (pH 3.6), fused-silica capillaries with 50.0 cm L_{tot} , 40 cm L_{eff} and 50 μm inside diameter and 375 μm outside diameter, separation at -20 kV , indirect detection at 254 nm, and samples injected hydrodynamically under 1 psi for 3 s. Control experiments with MG alone did not show the presence of formate or acetate.

with peroxynitrite alone showed the expected liberation of molecular oxygen, which was subtracted from the oxygen uptake curves obtained with the complete system. The total consumption of oxygen ($70 \pm 10 \mu\text{M}$; $n = 4$) by the reaction mixture containing 1.0 mM MG and 1.0 mM peroxynitrite in 200 mM phosphate buffer (pH 7.2) at 25 °C was not affected upon addition of nitrite (0.10–5.0 mM), a known contaminant of peroxynitrite stock solutions (33), and a product of peroxynitrate decomposition (41, 42). Formate and acetate ions were detected by CE as the main products in the final reaction mixtures maintained under continuous aeration for 30 min (Figure 3 and Table 1). The equipment was calibrated with a mixture of nitrite, nitrate, phosphate, glyoxalate, formate, and acetate (products predicted by the proposed schemes) at known concentrations, and oxalate was used as an internal standard. The absence of glyoxalate in the electropherogram strongly supports the notion that the MG carbonyl group most prone to nucleophilic attack is indeed the aldehydic (C1), not the MG ketonic group (C2). Both MG and peroxynitrite (each at 1 mM) produced 0.59 mM acetate and 0.48 mM formate, i.e., approximately 50% chemical yield of MG fragmentation to acetate and formate in a 1:1 ratio. Initial concentrations of 2.5 mM MG and 3.0 mM peroxynitrite

Table 1. Product Analysis of the Reaction of MG with Peroxynitrite^a

[MG] (mM)	1.00 mM ONOO ⁻	1.50 mM ONOO ⁻	3.00 mM ONOO ⁻	4.50 mM ONOO ⁻
1.00	0.59* 0.48#	0.59* 0.56#	0.79* 0.68#	0.78* 0.63#
2.50	0.70* 0.74#	0.79* 0.86#	0.89* 0.93#	1.06* 0.89#
10.0	0.71* 0.39#	0.85* 0.62#	1.04* 0.67#	1.44* 0.82#

^a CE was used to separate and quantify formate (*) and acetate (#) present in the reaction mixture (see the electropherograms in Figure 3).

yielded both products at ~0.90 mM (~30%). Upon addition of nitrite (0.25 and 0.50 mM; $n = 4$) to a mixture containing 1.0 mM MG and peroxynitrite, the yields of formate and acetate did not change significantly.

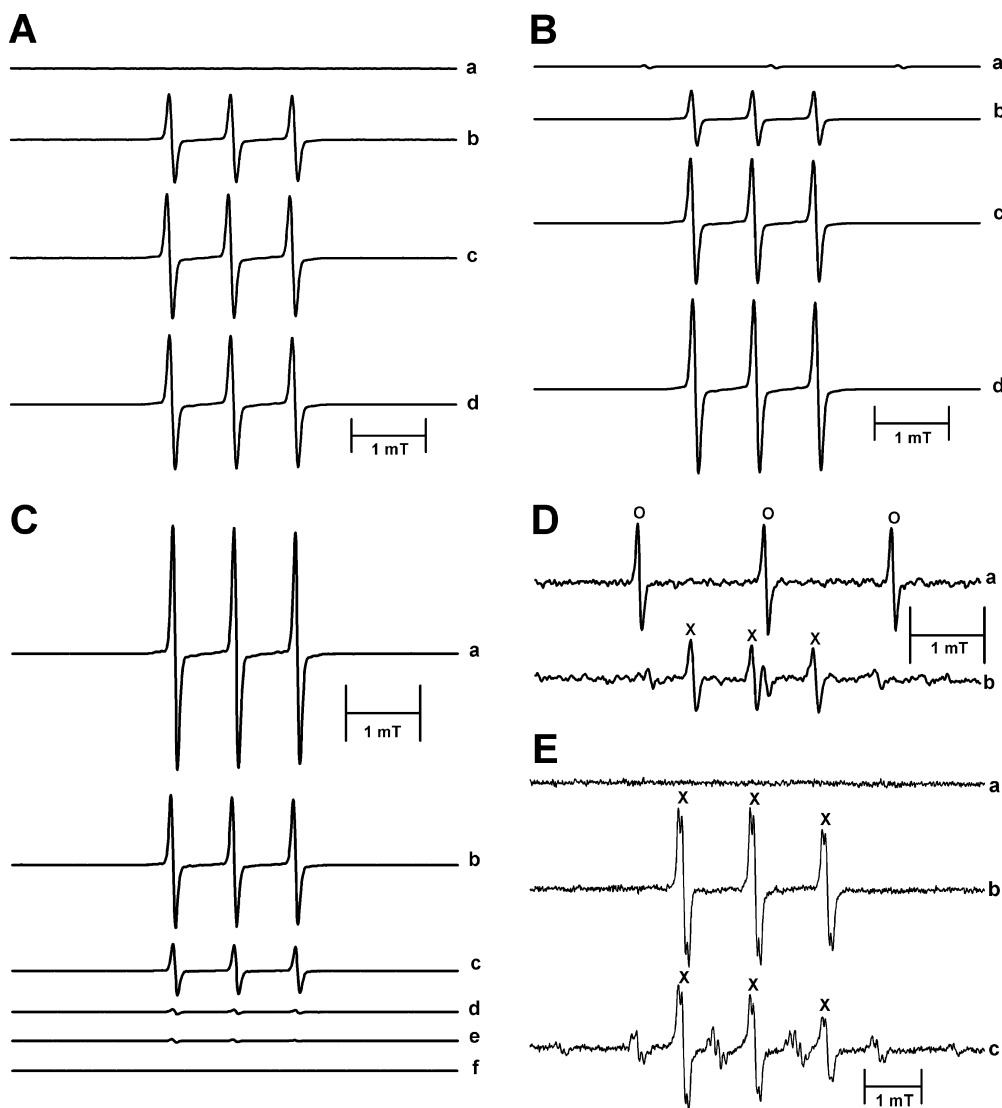


Figure 4. EPR spin trapping studies with MNP (20 mM) and DBNBS (10 mM) of the MG–peroxynitrite or hydrogen peroxide system in 250 mM phosphate buffer (pH 7.2) after incubation for 4 min at room temperature. (A) Spectra of a MNP–acetyl radical adduct obtained from peroxynitrite (1.5 mM) without (a) and with 5.0 (b), 10 (c), and 20 mM MG (d). (B) Spectra of MG (10 mM) without (a) and with 0.5 (b), 1.5 (c), and 2.5 mM peroxynitrite (d). For the MNP–acetyl adduct, a_N (observed) = 0.83 mT (for lit. NIEHS, $a_N = 0.78–0.83$). (C) Effect of carbonate on the amplitude of the EPR signal of the MNP–acetyl adduct obtained from MG (20 mM) and peroxynitrite (2.5 mM) without (a) and with 2.5 (b), 5.0 (c), 7.5 (d), 10.0 (e), and 12.5 mM sodium bicarbonate (f). (D) Incubation of MG with hydrogen peroxide: (a) MNP signal control and (b) reaction mixture containing 20 mM MG and 20 mM hydrogen peroxide. The signal marked O ($a_N = 1.72$ mT) is assigned to the di-*tert*-butylnitroxide signal (MNP contaminant) (43, 44) and the signal marked X ($a_N = 0.83$ mT) to the MNP–acetyl radical adduct. Minor undetermined carbon-centered radical signals are also detected, as reported by Nakayama et al. (45) in EPR studies with DBNBS, MG, and H₂O₂. (E) EPR spectra of a methyl radical adduct obtained with DBNBS after incubation of MG with peroxynitrite: (a) 20 mM MG (control), (b) 1.5 mM peroxynitrite (control), and (c) complete system. The signal marked X can be assigned to the oxidation product of DBNBS by peroxynitrite in the presence of sulfite that originated from DBNBS itself (48), whereas the other signal [$a_N = 1.42$ mT; $a_H = 1.34$ mT; $a_{H(m)} = 0.07$ mT] can be attributed to a methyl–DBNBS adduct (46, 47), which is expected to be the origin of three splittings from the three hydrogen atoms of the methyl group.

Important to note is the fact that the reaction samples for measuring the chemical yield of products were prepared as previously reported in a similar study with diacetyl (15), where care was taken via adjustment of the pH with phosphoric acid to keep the final pH between 7.1 and 7.5, and the oxygen concentration was not limiting because of the vigorous stirring of the reaction mixture.

EPR Spin Trapping Studies. EPR spin trapping studies with 20 mM MNP or 10 mM DBNBS were conducted in normally aerated MG-containing phosphate buffer upon treatment with peroxynitrite to possibly detect and identify carbon-centered radical intermediates.

In the presence of MNP, MG and peroxynitrite gave a triplet signal with an a_N of 0.83 mT that could be assigned to the MNP–acetyl radical adduct (for lit. NIEHS, $a_N = 0.78–0.83$

mT) (Figure 4A,B). The formyl radical adduct with MNP (for lit. NIEHS, $a_N = 0.7\text{--}0.77$ mT and $a_H = 0.14\text{--}0.25$ mT) was not detected in the EPR spectrum. The EPR signal was intensified with an increase in the concentrations of both MG (5–20 mM) and peroxynitrite (0.50–2.5 mM). That MG competes significantly with carbon dioxide for the peroxynitrite anion was indicated by the concentration-dependent quenching effect of added bicarbonate (2.5–12.5 mM) on the amplitude of the MNP triplet adduct signal obtained with 20 mM MG and 2.5 mM peroxynitrite (Figure 4C). The EPR signal was totally suppressed upon addition of bicarbonate at concentrations of >10 mM. Important to note is the fact that millimolar peroxynitrite can be replaced with H₂O₂ (20 mM) to generate the hypothetical MNP–acetyl radical adduct ($a_N = 0.83$ mT) (Figure 4D). Another signal could be assigned to di-*tert*-butylnitroxide ($a_N = 1.72$ mT), a contaminant frequently found in solutions of MNP (43, 44), and minor nonidentified signals appeared as well (Figure 4D). In this regard, it is important to note that Nakayama et al. (45) reported the occurrence of a DBNBS–methyl radical adduct, among minor nonidentified adducts, when treating MG with H₂O₂.

In turn, using DBNBS in the reaction of MG with peroxynitrite, the characteristic EPR signal corresponding to its methyl radical adduct appears: $a_N = 1.41$ mT; $a_H = 1.34$ mT; $a_{H(m)} = 0.07$ mT (Figure 4E) (46, 47). Methyl radical is predicted to be formed from the decarbonylation of acetyl radical and, less probably, from the fragmentation of a peroxonitroso adduct generated by the attack of peroxynitrite on C(2) of MG. If this were so, the counterfragment of MG oxidation, glyoxalate, should have appeared as a peak in the electropherogram of the spent reaction mixture. The signal present in the control experiment without MG ($a_N = 1.25$ mT; $a_H = 0.06$ mT) can be attributed to a DBNBS–SO₃^{•-} adduct (48) (Figure 4E).

CE-MS/MS Analysis of Acetylated L-Lysine. Panels A and B of Figure 5 depict the electropherograms of the final reaction mixture of 5.0 mM L-lysine, 10 mM MG, and 2.5 mM peroxynitrite monitored by the MS peak at m/z 147 (L-lysine) and m/z 189 (acetyl-L-lysine), respectively. The insets show the MS spectra of the corresponding electrophoretic peaks. The MS/MS fragmentation pattern of the ion at m/z 189.04 is shown in Figure 5C. The assignment of the MS/MS spectrum to an ϵ -*N*-acetyl-L-lysine adduct is supported by the following data. The [acetyllysine + H]⁺ species (m/z 189.04) is expected to undergo dehydration to form the ion at m/z 171 and subsequent decarbonylation to the ion at m/z 143, yielding an immonium fragment whose deamination renders the ion at m/z 126. Deacetylation of the immonium ion (–CH₂CO) then produces the fragment at m/z 84. The high abundance of the immonium fragments at m/z 143 and 126, according to Trelle and Jensen (49), is evidence of L-lysine acetylation in the ϵ -amino group, which is mechanistically unfavorable in the case of the α -isomer. Accordingly, had an α -*N*-acetyl-L-lysine adduct been produced, its protonated form would have lost a H₂CO₂ group and subsequently a CH₂CO group to yield an m/z 101 fragment. This fragment is, in fact, reported by the Spectral Database for Organic Compounds (MS-NW-7638 SDBS no. 22048) for α -*N*-acetyl-L-lysine, but it was not found in our samples. In addition, unidentified fragments at m/z 157 and 129 are present in the spectrum of the final reaction mixture, but not in the standard spectrum of α -*N*-acetyl-L-lysine.

Discussion

Nucleophilic addition of peroxynitrite to diacetyl in air-equilibrated phosphate has been shown to yield acetyl radical

(15, 16) and to acetylate L-histidine and dGuo added to the reaction mixture (15). This reaction raised the hypothesis that peroxynitrite and α -oxocarbonyls overproduced in metabolic situations such as inflammation in cellular sites might drive protein and DNA acetylation, thereby triggering adverse responses. We now studied MG, a metabolite putatively implicated in diabetes and other ketogenic disorders, as the electrophilic target for peroxynitrite, relying on the long-known higher reactivity of aldehydes compared to that of ketones. Nakayama et al. (45) recently reported that MG does, in fact, react with H₂O₂, yielding HO[•] and carbon-centered radicals, which was demonstrated by the use of EPR spin trapping with 5,5-dimethyl-1-pyrroline *N*-oxide (DMPO) and DBNBS. This reaction was shown to emit light in the presence of luminol, probably initiated by HO[•] radical (indirect chemiluminescence); however, the mechanism underlying the MG–H₂O₂ reaction was not clearly determined. Here, we have extended our studies on the MG–peroxynitrite system to the MG–H₂O₂ system, because an MG–H₂O₂ adduct could also undergo homolysis to an oxyl radical, although at a slower rate, and ultimately yield acetyl radical, which was not detected by Nakayama et al. (45). By analogy, Augusto et al. (50) have demonstrated that pyruvate reacts with both peroxynitrite and H₂O₂, yielding acetate and CO₂^{•-} radical.

The second-order rate constant for addition of peroxynitrite anion to MG is estimated here by stopped-flow kinetics to be approximately $1.0 \times 10^5 \text{ M}^{-1} \text{ s}^{-1}$ in 250 mM phosphate buffer (pH 7.2) at 25 °C (Figure 1). This value is higher than the values reported for diacetyl ($k_2 = 1.0 \times 10^4 \text{ M}^{-1} \text{ s}^{-1}$) (15) and HCO₃⁻/CO₂ ($k_2 = 3 \times 10^4 \text{ M}^{-1} \text{ s}^{-1}$), under similar experimental conditions (38, 39). The rate constants were calculated here from the experimental values, taking into consideration the actual concentrations of the free forms of MG in aqueous medium. Diacetyl and MG exist under dynamic equilibrium in aqueous medium with their mono- and dihydrate forms, where the dicarbonyl species are present at concentrations of only 23 and 1%, respectively (14, 16). The rate constant for phosphate-catalyzed dehydration of MG diol is several orders of magnitude lower than that of addition of peroxynitrite to MG (37). The hydration equilibrium constants are affected by the solvent's polarity, with the ratio of MG free to hydrate forms probably favoring the free, reacting species in hydrophobic, cell membrane environments.

Our experiments were performed at apparently nonphysiological concentrations. As the steady-state concentration of NO[•] in physiological systems falls in the nanomolar range, that of peroxynitrite formed by the diffusion-controlled reaction of NO[•] with superoxide anion radical is on the same order of magnitude. Indeed, estimates of the steady-state concentration of physiological CO₂-limited peroxynitrite by Ferrer-Sueta and Radi (22) are in the range 2–3 nM and often 2 orders of magnitude lower. Therefore, the pseudo-first-order rate constant for the reaction of MG with peroxynitrite ($k_2 \approx 1.0 \times 10^5 \text{ M}^{-1} \text{ s}^{-1}$) is expected to be in the range of $10^{-4}\text{--}10^{-6} \text{ s}^{-1}$. Considering that the MG reaction with plasma proteins displays rate values of $\sim 5 \times 10^{-5} \text{ s}^{-1}$ (2), reaction of MG with proteins may overwhelm that with peroxynitrite. In addition, although the k_2 value for the reaction of peroxynitrite with MG is 2–3 times higher than that with CO₂, one cannot disregard the presence of CO₂ in the physiological medium (1.3 mM) at much higher concentrations than MG (21). Nevertheless, it is tempting to propose that radical acetylation of biomolecules may take place chronically in vivo in specific microenvironments of tissues under adverse oxidative, nitrosative, and carbonyl stress. The pH profile of the

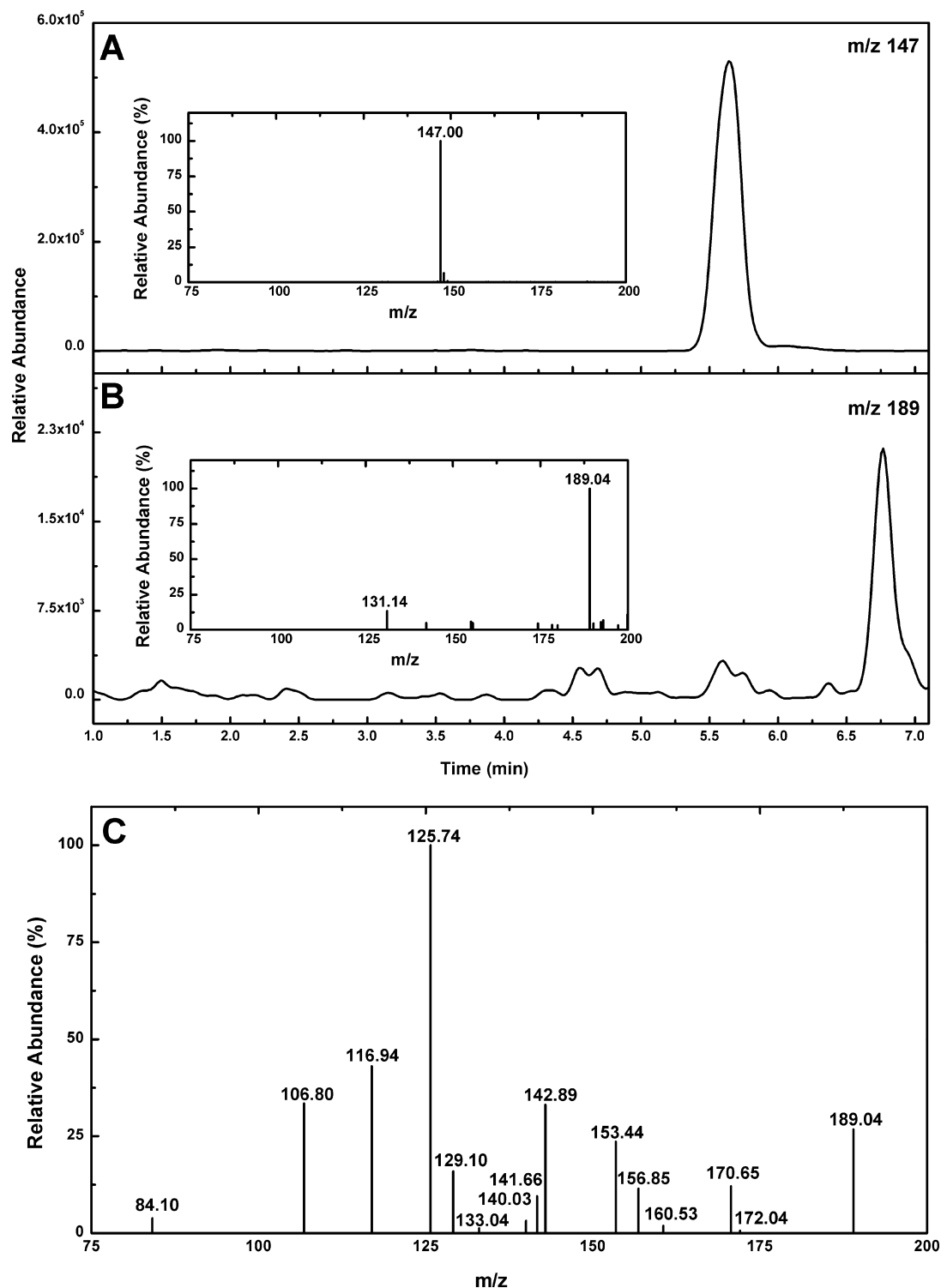


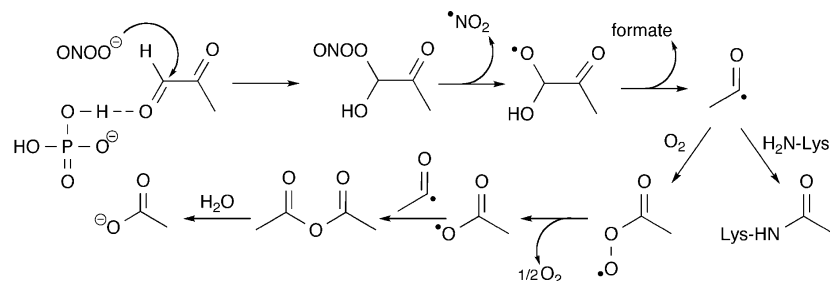
Figure 5. CE-MS/MS product analysis of L-lysine treated with the MG-peroxynitrite system. The reaction mixture consisted of 5.0 mM L-lysine, 10 mM MG, and 2.5 mM peroxynitrite in 200 mM phosphate buffer (pH 7.2). (A) Electropherogram traced at MS m/z 147 and (B) electropherogram traced at MS m/z 189. Insets show the MS spectra of corresponding electrophoretic peaks. (C) MS/MS of molecular ion at m/z 189, which can be attributed to 6N -acetyl-L-lysine formed by addition of the reaction-generated acetyl radical to the amino acid. Acetylated lysine was not detected in control experiments that included L-lysine alone, L-lysine with peroxynitrite, or L-lysine with MG.

MG-peroxynitrite reaction displays an ascending curve from lower pH toward neutrality, and then a long inflection resembling a plateau at pH \sim 7.2, which is followed by a sharp increase at alkaline pH values (Figure 1C). The ascendant portion of the curve may be attributed to increasing concentrations of the attacking peroxynitrite anion ($pK_a = 6.8$, tending to slightly higher values with increasing ionic strengths) (20) and to general acid catalysis of the nucleophilic addition to MG by the $H_2PO_4^-$ anion ($pK_a = 7.2$), but not by the conjugated

base HPO_4^{2-} . In agreement with a catalytic effect of phosphate anion on the MG-peroxynitrite reaction, the observed rate constants increase with an increase in buffer concentration (Figure 1D).

The MG reaction with peroxynitrite is accompanied by concentration-dependent oxygen uptake (Figure 2), ultimately forming acetate and formate ions (Figure 3 and Table 1), derived from oxidative fragmentation of the MG C(1)–C(2) bond. Pyruvate and glyoxalate ions were not detected in the electro-

Scheme 2. Mechanism of Acetylation of L-Lysine by the MG–Peroxynitrite System in Aqueous Medium



pherograms obtained from the spent reaction mixtures, thereby ruling out reactions involving direct oxidation of MG to pyruvate or attack of peroxynitrite on C(2) of MG leading to glyoxalate and formate ions. On the basis of previously reported works about the mechanism of addition of peroxynitrite to carbonyls such as ethanal and propanal (17), pyruvate and acetaldehyde (50, 18), and diacetyl-derived compounds (16) (diacetyl) (15, 16), we envisage the reaction as proceeding through the steps depicted by Scheme 1, probably route 1 as follows.

Following attack of the phosphate-catalyzed peroxynitrite anion on C(1) of MG, the nascent hypothetical nitrosoperoxy adduct undergoes O–O bond cleavage to form NO_2 and a MG-derived oxyl radical, whose β -scission yields acetyl radical and formate ion. Subsequent acetyl radical oxidation by molecular oxygen yields in acetate ion (Scheme 1). From classical photochemistry of carbonyl compounds, it is known that decarbonylation of acetyl radical to methyl radical (Norris type I photoreactions) is expected to occur. On the other hand, had the addition of peroxynitrite to MG unexpectedly occurred at the less reactive C(2) atom (route 2b of Scheme 1), glyoxalate anion should have been detected as one of the main products, which was not the case. Moreover, all attempts to detect formyl radical by spin trapping with MNP have failed. The fact that acetyl and methyl radicals can indeed be generated by the MG–peroxynitrite reaction is strongly suggested by EPR spin trapping experiments with MNP and DBNBS, respectively (Figure 4). Therein, EPR signals that can be attributed to the MNP–acetyl radical adduct ($a_N = 0.83$ mT) and to the DBNBS–methyl radical adduct [$a_N = 1.41$ mT; $a_H = 1.34$ mT; $a_{H(m)} = 0.07$ mT] were obtained. Methyl radical could also yield formate anion by dioxygen insertion followed by a Russell reaction (51). Significant competition between MG and CO_2 in the peroxynitrite reaction is indicated by quenching of the MNP–acetyl adduct signal upon addition of carbonate at relatively high concentrations (Figure 4C). This finding strengthens the hypothesis of the biological relevance of this reaction. Moreover, although much less reactive, H_2O_2 can replace peroxynitrite in the acetyl radical-generating reaction of MG (Figure 4D). Noteworthy in this respect is the fact that Nakayama et al. (45) previously reported that the MG– H_2O_2 system yields methyl radical and an unidentified carbon-centered radical that supposedly spark the chemiluminescence observed by the authors upon addition of luminol to the reaction mixture. Furthermore, our work may explain the mechanism underlying the formation of acetaldehyde and formate from D-lactate, an end product of the MG bypass, hyperproduced in rats fed dimethylaminoazobenzene-rich diets (52).

Altogether, the data reported here support a mechanism of MG oxidation by peroxynitrite and molecular oxygen to acetate and formate via an acetyl radical intermediate, which is initiated by nucleophilic addition of peroxynitrite to C(1) of MG (Scheme 1). Also, the acetylation activity of the MG–peroxynitrite system, previously reported using diacetyl/peroxynitrite and

L-histidine and dGuo as targets (15), was tested here on L-lysine (Scheme 2). The assignment of the MNP spin adduct to acetyl radical (Figures 4AB) was confirmed by the isolation and identification of ^6N -acetyl-L-lysine in the final reaction mixture by CE-MS. The hypothesis of post-translational acetylation of proteins by a radical mechanism, during normal or pathological events that lead to the accumulation of both MG and peroxynitrite, might be evoked as an additional pathway to acetyltransferase-catalyzed reactions. Further experiments are warranted to demonstrate this hypothesis. Epigenetic protein acetylations, especially in lysine residues of histones, have important consequences in cell signaling and regulation of the cell cycle (31).

Acknowledgment. This work was supported by grants from the Fundação de Amparo à Pesquisa do Estado de São Paulo (FAPESP), the Conselho Nacional de Desenvolvimento Científico e Tecnológico (CNPq), and the Instituto Nacional de Ciência e Tecnologia (INCT) Redoxoma. We thank Luiz H. Catalani and Wilhelm Baader (University of Sao Paulo, Sao Paulo, Brazil) and Brian Bandy (University of Saskatchewan, Saskatoon, SK) for a critical reading of the manuscript.

References

- (1) Kalapos, M. P. (1999) Methylglyoxal in living organisms: Chemistry, biochemistry, toxicology and biological implications. *Toxicol. Lett.* 110, 145–175.
- (2) Thornalley, P. J. (2005) Dicarbonyl Intermediates in the Maillard Reaction. *Ann. N.Y. Acad. Sci.* 1043, 111–117.
- (3) Kalapos, M. P. (2008) The tandem of free radicals and methylglyoxal. *Chem.-Biol. Interact.* 171, 251–271.
- (4) Thornalley, P. J. (2008) Protein and nucleotide damage by glyoxal and methylglyoxal in physiological systems: Role in ageing and disease. *Drug Metab. Drug Interact.* 25, 125–150.
- (5) Royer, L. O., Knudsen, F. S., de Oliveira, M. A., Tavares, M. F. M., and Bechara, E. J. H. (2004) Succinylacetone oxidation by oxygen/peroxynitrite: A possible source of reactive intermediates in hereditary tyrosinemia type I. *Chem. Res. Toxicol.* 17, 598–604.
- (6) Dutra, F., Ciriolo, M. R., Calabrese, L., and Bechara, E. J. H. (2005) Aminoacetone induces oxidative modification to human plasma ceruloplasmin. *Chem. Res. Toxicol.* 18, 755–760.
- (7) Deng, Y., Boomsma, F., and Yum, P. H. (1998) Deamination of methylamine and aminoacetone increases aldehydes and oxidative stress in rats. *Life Sci.* 63, 2049–2058.
- (8) House, J. D., Hall, B. N., and Brosnan, J. T. (2001) Threonine metabolism in isolated rat hepatocytes. *Am. J. Physiol.* 281, 1300–1307.
- (9) Thornalley, P. J. (1988) Modification of the glyoxalase system in human red blood cells by glucose *in vitro*. *Biochem. J.* 254, 751–755.
- (10) Nemet, I., Varga-Defterdarovic, L., and Turk, Z. (2006) Methylglyoxal in food and organisms. *Mol. Nutr. Food Res.* 50, 1105–1117.
- (11) Dhar, A., Desai, K., Liu, J., and Wu, L. (2009) Methylglyoxal, protein binding and biological samples: Are we getting the true measure? *J. Chromatogr., B: Anal. Technol. Biomed. Life Sci.* 877, 1093–1100.
- (12) Beisswenger, P. J., Howel, S. K., Touchette, A. D., Lal, S., and Szergold, B. S. (1999) Metformin reduces systemic methylglyoxal levels in type 2 diabetes. *Diabetes* 48, 198–202.
- (13) Nemet, I., Vijiã-Topiã, D., and Varga-Defterdarovic, L. (2004) Spectroscopic studies of methylglyoxal in water and dimethylsulfoxide. *Bioorg. Chem.* 32, 560–570.

- (14) Thornalley, P., Yurek-George, A., and Argirov, O. K. (2000) Kinetics and mechanism of the reaction of aminoguanidine with the α -oxoaldehydes glyoxal, methylglyoxal, and 3-deoxyglucosone under physiological conditions. *Biochem. Pharmacol.* **60**, 55–65.
- (15) Massari, J., Fujii, D. E., Dutra, F., Vaz, S. M., Costa, A. C. O., Micke, G. A., Tavares, M. F. M., Tokikawa, R., Assunção, N. A., and Bechara, E. J. H. (2008) Radical acetylation of 2'-deoxyguanosine and L-histidine coupled to the reaction of diacetyl with peroxynitrite in aerated medium. *Chem. Res. Toxicol.* **21**, 879–887.
- (16) Yang, D., Tang, T., Chen, J., Wang, X., Bartberger, M. D., Houk, K. N., and Olson, L. (1999) Ketone-catalyzed decomposition of peroxynitrite via dioxirane intermediates. *J. Am. Chem. Soc.* **121**, 11976–11983.
- (17) Uppu, R. M., Winston, G. W., and Pryor, W. A. (1997) Reactions of peroxynitrite with aldehydes as probes for reactive intermediates responsible for biological nitration. *Chem. Res. Toxicol.* **10**, 1331–1337.
- (18) Nakao, L. S., Ouchi, D., and Augusto, O. (1999) Oxidation of acetaldehyde by peroxynitrite hydrogen peroxide-iron(II). Production of acetate and methyl radicals. *Chem. Res. Toxicol.* **12**, 1010–1018.
- (19) Augusto, O., Bonini, M. G., Amanso, A. M., Linares, E., Santos, C. C., and Menezes, S. L. (2002) Nitrogen dioxide and carbonate radical anion: Two emerging radicals in biology. *Free Radical Biol. Med.* **32**, 841–859.
- (20) Lobachev, V. L., and Rudakov, E. S. (2006) The chemistry of peroxynitrite: Reaction mechanisms and kinetics. *Russ. Chem. Rev.* **75**, 375–396.
- (21) Medinas, D. B., Cerchiaro, G., Trindade, D. F., and Augusto, O. (2007) The carbonate radical and related oxidants derived from bicarbonate buffer. *IUBMB Life* **59**, 255–262.
- (22) Ferrer-Sueta, G., and Radi, R. (2009) Chemical biology of peroxynitrite: Kinetics, diffusion, and radicals. *ACS Chem. Biol.* **4**, 161–177.
- (23) Pacher, P., Beckman, J. S., and Liaudet, L. (2007) Nitric oxide and peroxynitrite in health and disease. *Physiol. Rev.* **87**, 315–424.
- (24) Szabó, C., Ischiropoulos, H., and Radi, R. (2007) Peroxynitrite: Biochemistry, pathophysiology and development of therapeutics. *Nat. Rev. Drug Discovery* **6**, 662–680.
- (25) Radi, R. (2004) Nitric oxide, oxidants, and protein tyrosine nitration. *Proc. Natl. Acad. Sci. U.S.A.* **101**, 4003–4008.
- (26) Ferrer-Sueta, G., Vitturi, D., Batinic-Haberle, I., Fridovich, I., Goldstein, S., Czapski, G., and Radi, R. (2003) Reactions of manganese porphyrins with peroxynitrite and carbonate radical anion. *J. Biol. Chem.* **278**, 27432–27438.
- (27) Goldstein, S., and Merényi, G. (2008) The chemistry of peroxynitrite: Implications for biological activity. *Methods Enzymol.* **436**, 49–61.
- (28) Rebrin, I., Bregere, C., Gallaher, T. K., and Sohal, R. S. (2008) Detection and characterization of peroxynitrite-induced modifications of tyrosine, tryptophan, and methionine residues by tandem mass spectrometry. *Methods Enzymol.* **441**, 283–294.
- (29) Ahmed, N., Babaei-Jadidi, R., Howell, S. K., Beisswenger, P. J., and Thornalley, P. J. (2005) Degradation products of proteins damaged by glycation, oxidation and nitration in clinical type 1 diabetes. *Diabetologia* **48**, 1590–1603.
- (30) Ahmed, N., Dobler, D., Dean, M., and Thornalley, P. J. (2005) Peptide mapping identifies hotspot site of modification in human serum albumin by methylglyoxal involved in ligand binding and esterase activity. *J. Biol. Chem.* **290**, 5724–5732.
- (31) Kouzarides, T. (2000) Acetylation: A regulatory modification to rival phosphorylation? *EMBO J.* **19**, 1176–1179.
- (32) Kaur, H., Leung, K. H. W., and Perkins, M. J. (1981) A water-soluble, nitroso-aromatic spin-trap. *J. Chem. Soc., Chem. Commun.* **3**, 142–143.
- (33) Beckman, J. S., Beckman, T. W., Chen, J., Marshall, P. A., and Freeman, B. A. (1990) Apparent hydroxyl radical production of peroxynitrite. Implications for endothelial injury from nitric oxide and superoxide. *Proc. Natl. Acad. Sci. U.S.A.* **87**, 1620–1624.
- (34) Beers, R. F., and Sizer, W. I. (1952) A spectrophotometric method for measuring the breakdown of hydrogen peroxide by catalase. *J. Biol. Chem.* **195**, 133–140.
- (35) Hughes, M. N., and Nicklin, H. G. (1968) Chemistry of pernitrites. I. Kinetics of decomposition of pernitrous acid. *J. Chem. Soc. A*, 450–452.
- (36) Gilbert, R. P., and Brandt, R. B. (1975) Spectrophotometric determination of methyl glyoxal with 2,4-dinitrophenylhydrazine. *Anal. Chem.* **47**, 2418–2422.
- (37) Betterton, E. A., and Hoffman, M. R. (1987) Kinetics, mechanism, and thermodynamics of the reversible-reaction of methylglyoxal (CH₃COCHO) with S(IV). *J. Phys. Chem.* **91**, 3011–3020.
- (38) Lyman, S. V., and Hurst, J. K. (1995) Rapid reaction between peroxynitrite ion and carbon dioxide: Implications for biological activity. *J. Am. Chem. Soc.* **117**, 8867–8868.
- (39) Uppu, R. M., Squadrito, G. L., and Pryor, W. A. (1996) Acceleration of peroxynitrite oxidations by carbon dioxide. *Arch. Biochem. Biophys.* **327**, 335–343.
- (40) Denicola, A., Freeman, B. A., Trujillo, M., and Radi, R. (1996) Peroxynitrite reaction with carbon dioxide/bicarbonate: Kinetics and influence on peroxynitrite-mediated oxidations. *Arch. Biochem. Biophys.* **333**, 49–58.
- (41) Gupta, D., Harish, B., Kissner, R., and Koppenol, W. H. (2009) Peroxynitrate is formed rapidly during decomposition of peroxynitrite at neutral pH. *Dalton Trans.*, 5730–5736.
- (42) Miyamoto, S., Ronsein, G. E., Corrêa, T. C., Martinez, G. R., Medeiros, M. H. G., and Di Mascio, P. (2009) Direct evidence of singlet molecular oxygen generation from peroxynitrate, a decomposition product of peroxynitrite. *Dalton Trans.*, 5720–5729.
- (43) Gunther, M. R., Peters, J. A., and Sivaneri, M. K. (2002) Histidinyl radical formation in the self-peroxidation reaction of bovine copper-zinc superoxide dismutase. *J. Biol. Chem.* **277**, 9160–9166.
- (44) Makino, K., Suzuki, N., Moriya, F., Rokushika, S., and Hatano, H. (1981) A fundamental study on aqueous-solutions of 2-methyl-2-nitrosopropane as a spin trap. *Radiat. Res.* **86**, 294–310.
- (45) Nakayama, M., Saito, K., Sato, E., Nakayama, K., Terawaki, H., Ito, S., and Kohno, M. (2007) Radical generation by the non-enzymatic reaction of methylglyoxal and hydrogen peroxide. *Redox Rep.* **12**, 125–133.
- (46) Gatti, R. M., Alvarez, B., Vasquez-Vivar, J., Radi, R., and Augusto, O. (1998) Formation of spin trap adducts during the decomposition of peroxynitrite. *Arch. Biochem. Biophys.* **349**, 36–46.
- (47) Royer, L. O., Knudsen, F. S., de Oliveira, M. A., Tavares, M. F. M., and Bechara, E. J. H. (2004) Peroxynitrite-initiated oxidation of acetoacetate and 2-methylacetoacetate esters by oxygen: Potential sources of reactive intermediates in keto acidoses. *Chem. Res. Toxicol.* **17**, 1725–1732.
- (48) Guo, R., Davies, C. A., Nielsen, B. R., Hamilton, L., Symons, M. C. R., and Winyard, P. G. (2002) Reaction of the spin trap 3,5-dibromo-4-nitrosobenzene sulfonate with human biofluids. *Biochim. Biophys. Acta* **1572**, 133–142.
- (49) Trelle, M. B., and Jensen, O. N. (2008) Utility of immonium ions for assignment of ϵ -N-acetylyllysine-containing peptides by tandem mass spectrometry. *Anal. Chem.* **80**, 3422–3430.
- (50) Vásquez-Vivar, J., Denicola, A., Radi, R., and Augusto, O. (1997) Peroxynitrite-mediated decarboxylation of pyruvate to both carbon dioxide and carbon dioxide radical anion. *Chem. Res. Toxicol.* **10**, 786–794.
- (51) Miyamoto, S., Ronsein, G. E., Prado, F. M., Uemi, M., Corrêa, T. C., Toma, I. N., Bertolucci, A., Oliveira, M. C., Motta, F. D., Medeiros, M. H. G., and Di Mascio, P. (2007) Biological hydroperoxides and singlet molecular oxygen generation. *IUBMB Life* **59**, 322–331.
- (52) Kitamura, Y., Kawase, M., and Ohmori, S. (2008) Formate excretion in urine of rats fed dimethylaminoazobenzene-rich diets: The possibility of formate formation from D-lactate. *Acta Med. Okayama* **62**, 193–203.

TX1002244